Published in final edited form as:
Cytometry A. 2014 May ; 85(5): 386–399. doi:10.1002/cyto.a.22452.

In Search of Antiaging Modalities: Evaluation of mTOR- and ROS/DNA Damage-Signaling by Cytometry

Zbigniew Darzynkiewicz[1,*], **Hong Zhao**[1], **H. Dorota Halicka**[1], **Jiangwei Li**[1], **Yong-Syu Lee**[2], **Tze-Chen Hsieh**[2], and **Joseph M. Wu**[2]

[1]Brander Cancer Research Institute and Department of Pathology, New York Medical College, Valhalla, New York 10595

[2]Department of Biochemistry and Molecular Biology, New York Medical College, Valhalla, New York 10595

Abstract

This review presents the evidence in support of the IGF-1/mTOR/S6K1 signaling as the primary factor contributing to aging and cellular senescence. Reviewed are also specific interactions between mTOR/S6K1 and ROS-DNA damage signaling pathways. Outlined are critical sites along these pathways, including autophagy, as targets for potential antiaging (gero-suppressive) and/or chemopreventive agents. Presented are applications of flow- and laser scanning- cytometry utilizing phospho-specific Abs, to monitor activation along these pathways in response to the reported antiaging drugs rapamycin, metformin, berberine, resveratrol, vitamin D3, 2-deoxyglucose, and acetylsalicylic acid. Specifically, effectiveness of these agents to attenuate the level of constitutive mTOR signaling was tested by cytometry and confirmed by Western blotting through measuring phosphorylation of the mTOR-downstream targets including ribosomal protein S6. The ratiometric analysis of phosphorylated to total protein along the mTOR pathway offers a useful parameter reporting the effects of gero-suppressive agents. In parallel, their ability to suppress the level of constitutive DNA damage signaling induced by endogenous ROS was measured. While the primary target of each of these agents may be different the data obtained on several human cancer cell lines, WI-38 fibroblasts and normal lymphocytes suggest common downstream mechanism in which the decline in mTOR/S6K1 signaling and translation rate is coupled with a reduction of oxidative phosphorylation and ROS that leads to decreased oxidative DNA damage. The combined assessment of constitutive γH2AX expression, mitochondrial activity (ROS, ΔΨPm), and mTOR signaling provides an adequate gamut of cell responses to test effectiveness of gero-suppressive agents. Described is also an in vitro model of induction of cellular senescence by persistent replication stress, its quantitative analysis by laser scanning cytometry, and application to detect the property of the studied agents to attenuate the induction of senescence. Discussed is cytometric analysis of cell size and heterogeneity of size as a potential biomarker used to asses gero-suppressive agents and longevity.

[*]Correspondence to: Dr Z. Darzynkiewicz, Brander Cancer Research Institute at NYMC and Department of Pathology, BSB 438, Valhalla, NY 10595. darzynk@nymc.edu.

Key terms

ribosomal protein S6 phosphorylation; cellular senescence; H2AX phosphorylation; DNA damage signaling; replication stress; translation; cell size; red cell distribution width; berberine; mitochondria

Mechanism of Aging: is it ROS or mTOR?

Erosion of telomeres at each cell division resulting in telomere dysfunction is the primary cause of irreversible cell cycle arrest defined also as intrinsic or replicative cellular senescence (Hayflick limit) (1–4). Whereas this event is the critical raison d'être of organismal aging and age-related mortality other factors contribute to aging as well. Premature cellular senescence considered to be unrelated to telomere shortening (3–5) is one of these factors. Among mechanisms inducing premature senescence are continuing cellular stress particularly the replication stress caused by oxidative DNA damage (4,5), activation of oncogenes (6), loss of tumor suppressor genes (7) and other causes of DNA damage (8,9). In fact, the persistent DNA damage by reactive oxygen species (ROS) generated in mitochondria during oxidative phosphorylation for a long time has been considered the primary mechanism of aging (ROS mechanism of aging) (10–16). The most deleterious lesions induced by ROS, the DNA double-strand breaks (DSBs), are repaired either by homologous recombination or nonhomologous DNA-end joining (NHEJ). The recombinatorial repair, which restores DNA integrity rather faithfully, requires DNA template and therefore can take place in cells that already have it replicated, i.e., in late S and G_2 phase cells. In cells lacking the template the repair is carried out by the error-prone NHEJ which may lead to base pairs deletion or rearrangement (17–19). When such defects occur at sites coding for an oncogene or tumor suppressor gene it may lead to somatic mutations predisposing to neoplasia. If they are at the telomeric DNA this may lead to a dysfunction of telomeres and replicative senescence (20–24). Accumulation of unrepaired or incorrectly repaired DNA lesions definitely lowers the genome integrity leading to loss of fidelity of transcription and generation of proteins with defective function.

It recently became a subject of intense dispute however whether the ROS mechanism is the key culprit of premature aging. The growing body of forthcoming evidence indicates that the constitutive activation of nutrient- and mitogen-signaling pathways rather than the ROS-induced DNA damage is the primary mechanism of aging (25–33). Activation of these pathways leads to enhanced translation, accumulation of proteins, cell growth in size and mass (hypertrophy), and cellular senescence. Particularly during the slowed down progression through the cell cycle, such as occurs during replication stress, the growth continues leading to the imbalance when the ratio of protein or RNA content to DNA increases, the cells grow in size and acquire the senescence (unbalanced growth) phenotype (34–36). The key players in this mechanism of aging are the insulin-like growth factors (IGFs) including the growth hormone (GH) (the "GH/IGFs axis"), AKT/PKB, and phosphoinositide 3-kinase (PI3K) pathways; their activation converges on mammalian target of rapamycin (mTOR) and its downstream substrate S6 protein kinase (S6K) (37–43) (Fig. 1). The perpetual activation of mTOR mediated by these signaling pathways is the driving force that leads to aging and senescence at the cellular and organismal level (mTOR

mechanism of aging). The most convincing evidence for the mTOR mechanism stems from the recently forthcoming results that show the increased lifespan and improved health-span of several kinds of organisms including mammals treated with the direct (rapamycin) or indirect (e.g., metformin) mTOR inhibitors (rapalogs) (30,32,44–53). There is also well documented evidence that impairment of signaling along the IGF-1/GH axis, upstream of mTOR, leads to increased longevity (54–59). Consistent with this mechanism are findings that overexpression of oncogenes and activation of the pathways upstream of mTOR accelerates cellular senescence and aging (6,60). On other hand, the evidence that anti-oxidants or other means of oxidative DNA damage prevention can extend the lifespan or distinctly reduce the symptoms of aging, with a few exceptions (15,16), is scarce (reviewed in Ref. 28).

Antiaging Strategies—Attenuation of mTOR/S6 Signaling and ROS–DNA Damage; Activation of Autophagy

Figure 1 illustrates the mTOR/S6 pathways associated with cellular senescence and aging and their linkage with the ROS-DNA damage signaling pathways. It also points out the targets for potential antiaging (gero-suppression) as well as chemopreventive modalities along these pathways. Results of our experiments reviewed further in the present article are strongly consistent with this representation. The primary targets for gero-suppression are the signaling pathways upstream of mTOR (mTORC1; raptor), that include the IGF-1/GH axis, MAPK, AKT, and PI3K; they are activated by mitogens, growth factors, sugars and amino acids. Their signaling can be suppressed by calorie restriction mimetics such as 2-deoxy-d-glucose and by inhibitors of mitogens and growth factors, primarily of somatotropin (growth hormone, GH) and IGF-1 (54–56). The strongest evidence of gero-suppression by targeting GH and IGF-1 provide findings of extended health-span and life-span of mammals having mutations that reduce GH and IGF-1 signaling (57,58).

Downstream of these signals, the kinase activity of mTOR (raptor) is directly suppressed by its specific inhibitor, rapamycin. The evidence that rapamycin has gero-suppressive properties is so persuasive (50–52,59,61–63) that it prompted some authors to advice its instant implementation as an human antiaging drug/supplement extending the lifespan, preventing the age-associated diseases and reducing costs of health care (64). Indirect inhibition of mTOR is achieved through activation of AMPK (41). Metformin and berberine are among its activators that have been shown to have gero-suppressive properties. Both these drugs are effective to treat diabetes type 2. Their mechanism of AMPK activation involves inhibition of electron transport chain in mitochondria that leads to a decline in content of ATP, an increase of AMP/ATP ratio and thus provides the trigger activating AMPK. There is ample evidence of the gero-suppressive properties of metformin (44–48). Particularly convincing are results of recent experiments showing extended longevity and health-span of mice fed with this drug (44,47,48). Similar as in the case of rapamycin (64), with its long-term clinical usage and already well-known pharmacokinetics and toxicity profile, the use of metformin as an antiaging drug has been recently postulated (65). Berberine, a naturally occurring alkaloid with a long history of medicinal use in both Ayurvedic and old Chinese medicine, was also shown to have antiaging properties and

found to be effective in treatment of several age associated diseases (66–71). We have recently reported that both metformin (72) and berberine (73) suppress mTOR signaling as evidenced by the reduced level of constitutive phosphorylation of the ribosomal protein S6 (RP-S6) on Ser235/236, the key effector of the mTOR/S6K1 signaling, measured in individual cells by flow and laser scanning cytometry. Similar approach, namely reduction of phosphorylation of RP-S6, measured ex vivo in T lymphocytes by cytometry, has also been used to monitor effectiveness of mTOR inhibitors used clinically as immuno-suppressors (74).

Activation of autophagy plays also significant role as another gero-suppressive mechanism (75–82). The autophagy-associated genes were shown to be critical for longevity of different organisms from yeasts, flies, nematodes up to mice. There is also convincing evidence that induction of autophagy leads to extension of the lifespan while inhibition of autophagy has the opposite effect. Polyamines, particularly spermidine, are among the most effective inducers of autophagy (78–81). Interestingly, autophagy is often activated in association with suppression of signaling along the IGFs and mTOR pathways and inhibitors of these pathways (e.g., rapamycin) are widely used as inducers of autophagy (80–83). Activation of autophagy is also triggered during caloric restriction (80). The gero-suppressive properties of resveratrol, the widely popularized “health benefiting” supplement, are considered to be mediated by activation of SIRT-1, the member of sirtuins, the family of NAD+-dependent protein deacetylases, which also are associated with induction of autophagy (78,79). Activation of sirtuins triggers deacetylation of histones and transcription factors silencing several genes that regulate stress, metabolism, and survival pathways. It should be noted, however, that as yet neither there is a definite evidence of life extension of vertebrates by resveratrol nor of its antiaging properties in human (84).

The scheme presented in Figure 1 illustrates also a special relationship between the gero-suppressive versus chemopreventive properties of the agents targeting ROS and/or mTOR. Persistent activation of mTOR/S6 pathway is associated with translation that requires constant generation of ATP that involves oxidative phosphorylation which leads to formation of ROS and oxidative DNA damage. The damage of oncogenes or tumor suppressor genes can lead to neoplastic transformation. Consistent with this are observations that antioxidants have chemopreventive properties (85). While they have relatively minor impact on longevity (reviewed in Refs. 28 and 86) their potential gero-suppressive properties cannot be disregarded in light of the evidence that oxidative DNA damage of telomeric DNA as well as lipid peroxidation are among the factors driving the aging process (20–24). On other hand, the rapalogs because of their effect on suppression of translation as well as on ROS production demonstrate both the gero-suppressive as well as chemopreventive properties (86–90).

Effect of the Reported Gero–Suppressive Agents on Constitutive DNA Damage Response and Abundance of ROS

We have previously reported that constitutive DNA damage response (CDDR) in the untreated normal or tumor cells, detected as the “background” level of expression of histone H2AX phosphorylated on Ser139 (γH2AX) and of activated *Ataxia Telangiectasia-mutated*

protein kinase (ATM) phosphorylated on Ser1981, is a reporter of the ongoing DNA damage induced by endogenous ROS, the by-products of oxidative phosphorylation (91–93). These phosphorylation events were detected with phospho-specific antibodies (Ab) and measured by flow- or laser scanning-cytometry. Variety of tests has been made to ascertain that CDDR is indeed caused by the endogenous oxidants. Thus, the level of CDDR was suppressed, in a concentration-dependent relationship, in cells treated with the classical ROS scavenger N-acetylcysteine (93) or with another scavenger, hyaluronate (94). It was also markedly reduced in cells growing in hypoxia as well as when treated with several agents considered to have either antioxidant properties such as ascorbate and celecoxib or by suppressing cellular metabolic activity and oxidative phosphorylation by treatment with the calorie mimetic agent 2-deoxy-d-glucose (95), or with 3-bromopyruvate, the inhibitor of glycolysis (92). On other hand, activation of metabolic activity, e.g., in the course of mitotic stimulation of lymphocytes dramatically elevated the level of expression of γH2AX and activation of ATM (96).

Having established that the constitutive (background) level of DNA damage response to a large extent is a reporter of DNA damage by endogenous oxidants several drugs reported as having antiaging and/or chemopreventive properties, were tested with respect to their capability to attenuate the level of constitutive expression of γH2AX and activation of ATM (72). Among the tested drugs/supplements were: 2-deoxy-d-glucose (2dG) (97–99), metformin (MF) (44–49,53), rapamycin (RAP) (50–52), berberine (BRB) (100–104), 1,25-dihydroxyvitamin D3 (Vit. D3) (105–108), resveratrol (RSV) (79,109–115), and acetylsalicylic acid (aspirin) (ASA) (116–121).

Figure 2 illustrates the effect of exposure of human lymphoblastoid TK6 cells for 24 h to the reported antiaging agents on the level of constitutive expression of γH2AX (72). The expression of γH2AX shows cell cycle specificity being higher in G_2 and late S compared to G_1 phase cells. It is distinctly evident that the expression of γH2AX in cells treated with each of the agents was decreased and the decline was approximately of similar magnitude regardless of the cell cycle phase. The highest degree of γH2AX reduction (>50%) was seen in the cells treated with 2dG and RAP. The treatment with nearly all these drugs had no apparent effect on the cell cycle distribution; the exception were cells treated with 50 nM RAP which show about 50% reduction in frequency of cells in S and G_2M (marked by the arrow in the DNA histogram), consistent with a partial arrest in G_1 phase of the cell cycle. In the drug-treated cultures, there was no evidence of cell death either by the mode of necrosis or apoptosis. While exposure to these agents for 4 h led to relatively minor (<15%) decline in γH2AX, the treatment for 48 h had similar effect as for 24 h (72). More detailed assessment of the effects of MF (122), Vit. D3 (123), and the biscoclaurine alkaloid cepharanthine (124) in terms of their capability to reduce the level of constitutive activation of ATM and of phosphorylated γH2AX, including the time and dose responses to these agents, have been published separately. In light of the recently revealed properties of MF to enhance the health-span and life-span of several organisms including mice (44,47,48,65) of particular interest were observations of the decline of γH2AX in cells treated with this drug.

The reduction of DNA damage signaling by the gero-suppressive agents revealed by the suppression of γH2AX was paralleled by a drop in the level of endogenous ROS (Fig. 3).

The data show that the exposure of TK6 cells to each of these agents led to a marked decrease in cells ability to oxidize 7'-dihydrodichlorofluorescein–diacetate (H_2DCF-DA); its oxidation results in formation of the strongly fluorescent DCF which is considered to be a marker of endogenous ROS abundance (125) (top panels of Fig. 3). The most effective in reducing the ROS level were BRB, Vit. D3, RSV, and ASA. Bottom panels of Figure 3 illustrate the treatment-induced changes in electrochemical transmembrane potential of mitochondria ($\Delta\Psi$m) revealed by accumulation of the mitochondrial probe rhodamine 123 (Rh-123), the marker of energized mitochondria (126,127). The reduction of Rh-123 binding was seen in cells exposed to each of these agents, and was the most pronounced after treatment with RAP (72). However, the overall degree of reduction of $\Delta\Psi$m was of a lesser magnitude compared to the decline of ROS abundance.

It should be noted that BRB binds to mitochondria and shows weak fluorescence (73). This fluorescence has no effect on measurement of γH2AX or RP-$S6^P$, because it is totally released from the cells following their fixation. However, in the nonfixed cells, even in the presence of this fluorochrome, the decrease in intensity of Rh123 as well as of DCF was observed in the BRB-treated cells, indicating that a weak BRB fluorescence was more than overcompensated by Rh123 or DCF fluorescence so a decrease of the latter could be observed (73).

Reduction of mTOR Signaling by the Gero–Suppressive Agents

As mentioned earlier, phosphorylation of ribosomal protein S6 (RP-S6), the downstream target of mTOR activation, is a sensitive gauge that reports the level of protein synthesis considered to the key element driving the aging process. The effect of exposure of TK6 cells to the investigated gero-suppressive agents on level of phosphorylation of RP-S6 is shown in Figure 4. Unlike γH2AX, neither in control nor in the drug-treated cells the phosphorylation of RP-S6 shows significant differences related to cell cycle phase; somewhat higher expression of RP-$S6^P$ in S and G_2M compared to G_1 cells reflects an overall increase in cell size during progression through cell cycle. It is quite evident however that the treatment with each of these antiaging agents led to a decrease in the level of phosphorylated S6 protein. The most dramatic decrease (>95%) was seen in the cells treated with RAP. The cells treated with 2dG showed the least degree of the decrease (32–38%). There was no evidence that treatment of TK6 cells with all these drugs for 4 h had any distinct effect on the cell cycle progression as detected by analysis of DNA content frequency histograms (not shown).

To confirm and extend the findings obtained by cytometry we assessed also the effects of gero-suppressive agents on mTOR signaling by Western blotting (72; Fig. 5). Having available phospho-specific Abs that detect phosphorylation of mTOR and the eukaryotic translation initiation factor 4E–binding protein (4EBP1) in addition to RP-S6 applicable to Western blotting (not yet available for cytometry) we have been able to test the level of phosphorylation of these proteins as well. Phosphorylation of 4EBP1, similar to that of RP-S6, is a gauge of a rate of translation (37–41). Exposure of cells to the gero-suppressive agents lowered phosphorylation of mTOR concurrently with its downstream targets RP-S6 and 4EBP1 (Fig. 5). The most pronounced and consistent effect was seen in the case of RP-

S6 where the level of phosphorylation of this protein was reduced by each of the studied agents, most extensively by 95, 78, and 70%, by RAP, BRB, and 2dG, respectively. RAP, BRB, 2dG, and Vit. D3 were also quite effective in lowering the level of $4EBP1^P$, by 52, 51, 51, and 25%, respectively, whereas RSV and ASA had no such effect.

Attenuation of the constitutive level of RP-S6 phosphorylation by the gero-suppressive agents listed in Figures 2–5 was also observed in human pulmonary adenocarcinoma A459 and in diploid WI-38 fibroblasts as well as in mitogenically stimulated human lymphocytes exposed to these agents (72). Fluorescence of the first two cell types was measured by laser scanning cytometry while that of lymphocytes by flow cytometry (72). Thus, the observed effect of these gero-suppressive agents is not related to a particular cell type and is observed both in normal and tumor cells.

Ratiometric Analysis of Phosphorylated to Total Protein Content Along the mTOR Signaling

The results reporting effects of the studied drugs on the “total” mTOR, RP-S6, and 4EBP1 protein content shown in Table 1 were particularly interesting when compared with the changes in “ratio” of the phosphorylated protein fraction to the “total content” of the respective protein. They show that exposure of cells to each drug led to a distinct upregulation of mTOR and 4EBP1. It was not the case of RP-S6, which with an exception of 2dG and BRB, showed a minor decline. However, compared with the apparent increase of total protein content, the level of the phosphorylated fractions of the respective protein was more severely reduced. This overcompensated upregulation of the content and is reflected by the reduction of the ratio of “phosphorylated to total content” of the respective proteins. In the case of RP-S6 and 4EBP1, the downstream targets of mTOR driving the translation rate, the most effective was BRB and RAP, reducing proportion of the phosphorylated to total protein content by 75 and 72%, respectively (Table 1).

The apparent discrepancy of the effects of the studied drugs in terms of a decrease of expression of $RP\text{-}S6^P$ when compared with no change, or even an increase, in expression of phosphorylated mTOR or 4EBP1 (e.g., in the case of Vit. D3, RSV, or ASA) may be due that there are parallel signaling pathways, not necessarily solely of mTOR, which affect the level of phosphorylation of RP-S6 (37–41). These data also point out that the level of RP-S6 phosphorylation may be the more sensitive for detecting the effectiveness of potential anti-aging drugs compared with mTOR or other upstream signaling pathways.

The data of Western blotting (Fig. 5, Table 1) point out the importance of ratiometric analysis of the phosphorylated to total protein. In our earlier studies we have introduced this approach to examine the degree of phosphorylation of retinoblastoma gene product (pRb) by flow cytometry using the phospho-specific Ab and measuring the ratio of phosphorylated to total protein content (129,130). Figure 6 presents our recent data showing the effect of BRB, one of gero-suppressive agents (100–104), on the ratio of phosphorylated to total RP-S6 protein in A549 cells. The concentration–dose reduction in the degree of phosphorylation of this protein is much evident as the ratio $RP\text{-}S6^P/RP\text{-}S6^T$ decreases stepwise in the cells treated with 5–60 μM BRB concentration range. These plots also demonstrate very large

heterogeneity between individual cells in the ratio of phosphorylated to total RP-S6 but essentially no cell cycle-phase difference. The data emphasize the possibility offered by cytometry to assess the ratio of phosphorylated to total proteins along the mTOR signaling, by allowing the detection of cell heterogeneity in populations, and through gating analysis, correlating this ratio with other cell attributes, e.g., such as DNA content viz. the cell cycle position. This capability is expected to be of particular value in further studies of possible effectiveness of potential gero-suppressive agents.

Attenuation of Premature Cellular Senescence

As mentioned earlier, the premature cellular senescence is considered to be one of the factors driving the aging process and persistent replication stress is the primary mechanism contributing to the induction of premature cell senescence (3,4,9,36). The most characteristic feature of cells undergoing senescence is their increase in size and change in morphology marked by their dramatic “flattening” appearance, combined with distinctly reduced cell density at plateau phase of growth (131). It is possible that increased adherence to substratum may contribute to the observed “flattening.” We have developed a cytometric approach to assess the depth of cellular senescence by measurement of these morphometric changes concurrently with other markers of senescence by laser scanning cytometry (LSC) (132,133). Figure 7 illustrates features of A549 cells induced to senescence by treatment with 2 nM concentration of mitoxantrone (Mxt). This drug, targeting DNA topoisomerase II, at such low concentration induces persistent replication stress that manifests by DNA damage signaling, such as expression of γH2AX, and ultimately reduces the frequency of cells progressing through S. The morphometric analysis of the nucleus stained with the DNA fluorochrome DAPI shows an increase in nuclear area concomitant with the decrease in intensity of DAPI maximal pixel fluorescence (132,133). The latter is a consequence of cell flattening which makes the nucleus very thin. The integral of intensity of DAPI fluorescence over the nucleus reports DNA content and thus the cell cycle phase, which as seen in Figure 7 (insets) indicates cell arrest in G_1 and G_2M with paucity of S-phase cells in the Mxt-treated cultures. As nuclear area in senescent cells is increased and DAPI maximal pixel decreased the ratio of maximal pixel to the area (Mp:area) provides an even more sensitive marker reporting this change in cell morphology than either of these measurements alone (Fig. 7B). The cells arrested in G_1 and G_2M in the Mxt-treated cultures show a 10- to 19-fold increase in expression of the CDK inhibitor $p21^{WAF1}$, another marker of cellular senescence (3,131–133). Activation of the senescence-associated β-galactosidase (SA-β-gal) considered the hallmark of cellular senescence (3,131) measured by LSC by light absorption of the SA-β-gal product was also markedly elevated in cells growing in the presence of Mxt (132–134). In cells growing with Mxt for 48 and 72 h, respectively, the SA-β-gal activity when expressed as percent of the enzyme-positive cells was increased from 1.4 to 18 and 41% and when expressed as the mean value of the light absorption, from 1.0 by 7.4- and 14.7-folds (Figs. 7D and 7E). Very similar changes in all these parameters were also observed in A549 cells treated with low concentration of another DNA damaging (crosslinking) drug, mitomycin C (134). The data thus reflect that persistent DNA replication stress induced at low concentration of these DNA damaging drugs when

combined with suppression of cell proliferation (G_2 arrest) leads to development of a classical senescence phenotype.

This model of Mxt-induced cellular senescence has been used to test gero-suppressive agents as to whether their inclusion into the cultures together with the DNA-damaging drug can attenuate the induction and progression of the senescence phenotype. Figure 8 illustrates the effect different concentration of BRB, added into the cultures of A549 cells treated with Mtx, on the morphometric changes as measured by nuclear area (area) and maximal pixel (Mp) of DAPI fluorescence as well as on expression of p21, γH2AX, and RP-$S6^P$. The Mxt-induced senescence of these cells manifested in over 70% reduction of Mp:area ratio, a dramatic increase in expression of p21 (34.5-fold), 3.5-fold increase in expression of γH2AX and over 10% decrease in RP-$S6^P$. However, in the cells that were treated with Mxt in the presence of BRB the increase of all these markers of senescence was distinctly reduced, in a concentration-dependent mode. At the highest (60 μM) BRB concentration the Mp:area ratio was increased by 182%, expression of p21 was decreased by 94%, of γH2AX by 52%, and of RP-$S6^P$ by 81% compared to cells treated with Mxt alone. The induction of p21 by Mxt was paralleled by cell arrest in G_2M, and the degree of arrest was to a certain extent, reduced at 5 and 10 μM BRB concentration. The induction SA-β-gal activity by Mxt was also significantly prevented at all concentrations of BRB (73). Using the same model of experiment as presented in Figure 8, attenuation of the Mxt-induced cellular senescence was also observed when the cells were treated with this drug in the presence of MF and/or RAP but not of Vit. D3 or RSV (data not shown).

Cytometric Analysis of Cell Size and Heterogeneity, a Potential Biomarker of Gero–Suppressive Agents and Longevity

As mentioned earlier one of outcomes of replication stress when paralleled by the continuing translation driven by mTOR/S6 signaling is growth imbalance characterized by the increased cell size and increased protein to DNA ratio (34–36). Cell size can be easily assessed by cytometry either through the Coulter volume or forward light scatter measurement. The increased forward light scatter was shown to be a marker of senescence of variety of cell types, including normal fibroblasts and cancer cell lines (135,136). It should be noted however that human T lymphocytes induced to replicative senescence by continuing growth in vitro show no measurable increase in size (137) indicating that cell size increase while typical for many cell types cannot be considered a fundamental marker of cellular senescence, or at least not in the case of replicative senescence. The reduction of cell size, on the other hand, occurs during cell treatment with gero-suppressive agents. Figure 9 presents a decrease in forward light scatter (FLS), considered to a marker of cell size (138,139), of TK6 cells exposed to different concentration of BRB measured concurrently with a decrease in phosphorylation of RP-S6. While the decrease in FLS is of similar degree for cells in all phases of the cell cycle, the reduction of RP-S6 phosphorylation is of somewhat higher extent in S and G_2 cells than in G_1 cells.

Of particular interest in area of aging/longevity and flow cytometry are tantalizing observations, overlooked in the literature pertaining cytometry, that the red blood cell distribution width (RDW) is remarkably strong predictor of longevity, including all causes

of death, for adults aged 45 years and older (140). The RDW is a measure of heterogeneity of size of erythrocytes, expressed as coefficient of variation (CV) of the mean value of the erythrocyte Coulter volume, routinely reported in a standard complete blood count, and increased in certain types of anemia. However, this predictor remains strongly associated with mortality even after excluding all types of red cell blood diseases or other conditions that can affect red blood cells, e.g., such as vitamin B12 deficiency (140). Incredibly, the persons with the bottom quintile of the CV (<12.60%) at age ≥65 have over 60% longer survival after12 years compared to persons with the top quintile (>14.05%). It is tempting to speculate that IGFs/mTOR signaling is one of the factors, if not the key factor, that plays a role in the observed correlation between the RDW and mortality. In support of this contention are the data that IGF-1 can enhance erythropoiesis by activation of erythropoietin (141–144) and also can affect the final stages of erythroid maturation (145). The IGFs/mTOR signaling dramatically affects the cell size as shown in the case of 32D-derived myeloid cells which were 50% smaller after having deleted IGF-1 receptor (146). It is possible there-fore that persistent activation of erythropoiesis through IGF-1/mTOR signaling leads to heterogeneity of erythrocyte sizes because of their higher turnover rate. Further support to this contention provide recent findings by Kozlitina and Garcia (147) on the association between telomere length, size of erythrocytes, and RDW, which show that persons having short telomeres have increased fraction of larger red cells and most importantly, increased heterogeneity of their sizes revealed by RDW. However, while there is an association between the level of IGF-1 in serum and telomere length it is unclear whether there are mechanistic bases for this association (148,149). Given the above, the easily measured RDW may be a useful biomarker of the constitutive level of IGF-1 signaling, the critical factor accountable for longevity (54–59). As it is the subject of analysis using Coulter volume or forward light scatter, it should be of notice and importance in field of cytometry. It is possible that heterogeneity of other easily accessed cell types (e.g., other blood cells) may also be associated with constitutive level of IGFs/mTOR signaling and longevity. These tantalizing findings, however, have to be reproduced in further studies and mechanism of this phenomenon, whether linking it with the IGFs/mTOR signaling or not, explained.

This review does not cover the role of telomeres length, which is the critical marker of replicative senescence (1–5), plays a role in premature senescence and can be assessed by flow and imaging cytometry (150–152). Several recent review articles have discussed this subject (153–157). Although there are several cytometric methods to detect autophagy and lysosomal activity (155–158) and, as mentioned, autophagy is of importance in aging and in discovery of gero-suppressive agents (75–83,159–161), application of these methods in such studies is also not covered by the present review.

Literature Cited

1. Hayflick L, Moorhead PS. The serial cultivation of human diploid cell strains. Exp Cell Res. 1961; 25:585–621. [PubMed: 13905658]
2. Harley CB, Futcher AB, Greider CW. Telomeres shorten during ageing of human fibroblasts. Nature. 1990; 345:458–460. [PubMed: 2342578]
3. Rodier F, Campisi J. Four faces of cellular senescence. J Cell Biol. 2011; 192:545–556.

4. Mathon NF, Lloyd AC. Cell senescence and cancer. Nat Rev Cancer. 2001; 1:203–213. [PubMed: 11902575]
5. Sherr CJ, DePinho RA. Cellular senescence: Mitotic clock or culture shock? Cell. 2000; 102:407–410. [PubMed: 10966103]
6. Serrano M, Lin AW, McCurrach ME, Beach D, Lowe SW. Oncogenic ras provokes premature cell senescence associated with accumulation of p53 and $p16^{INK4a}$. Cell. 1997; 88:593–602. [PubMed: 9054499]
7. Chen Z, Trotman LC, Shaffer D, Lin HK, Dotan ZA, Niki M, Koutcher JA, Scher HI, Ludwig T, Gerald W, et al. Crucial role of p53-dependent cellular senescence in suppression of Pten-deficient tumorigenesis. Nature. 2005; 436:725–730. [PubMed: 16079851]
8. Gerwitz DA, Holt SE, Elmore LW. Accelerated senescence: An emerging role in tumor cell response to chemotherapy and radiation. Biochem Pharmacol. 2008; 76:947–957. [PubMed: 18657518]
9. Litwiniec A, Grzanka A, Helmin-Basa A, Gackowska L, Grzanka D. Features of senescence and cell death induced by doxorubicin in A549 cells: Organization and level of selected cytoskeletal proteins. J Canc Res Clin Oncol. 2010; 36:717–736.
10. Barzilai A, Yamamoto K. DNA damage responses to oxidative stress. DNA repair (Amst). 2004; 3:1109–1115. [PubMed: 15279799]
11. Moller P, Loft S. Interventions with antioxidants and nutrients in relation to oxidative DNA damage and repair. Mutat Res. 2004; 551:79–89. [PubMed: 15225583]
12. Beckman KB, Ames BN. Oxidative decay of DNA. J Biol Chem. 1997; 272:13300–13305.
13. Vilenchik MM, Knudson AG. Endogenous DNA double-strand breaks: Production, fidelity of repair, and induction of cancer. Proc Natl Acad Sci USA. 2003; 100:12871–12876. [PubMed: 14566050]
14. Karanjawala ZE, Lieber MR. DNA damage and aging. Mech Ageing Dev. 2004; 125:405–416. [PubMed: 15272504]
15. Schriner SE, Linford NJ, Martin GM, Treuting P, Ogburn CE, Emond M, Coskun PE, Ladiges W, Wolf N, Van Remmen H, Wallace DC, Rabinovitch PS. Extension of murine life span by over expression of catalase targeted to mitochondria. Science. 2005; 308:1875–1878. [PubMed: 15976292]
16. Parrinello S, Samper E, Krtolica A, Goldstein J, Melov S, Campisi J. Oxygen sensitivity severely limits the replicative lifespan of murine fibroblasts. Nat Cell Biol. 2003; 5:741–747. [PubMed: 12855956]
17. Jeggo PA, Lobrich M. Artemis links ATM to double strand end rejoining. Cell Cycle. 2005; 4:359–362. [PubMed: 15684609]
18. Seluanov A, Mittelman D, Pereira-Smith OM, Wilson JH, Gorbunova V. DNA end joining becomes less efficient and more error-prone during cellular senescence Proc Natl Acad Sci USA. 2004; 101:7624–7629.
19. Bogomazova AN, Lagarkova MA, Tskhovrebova LV, Shutova MV, Kiselev SL. Error-prone nonhomologous end joining repair operates in human pluripotent stem cells during late G2. Aging (Albany). 2011; 3:584–596.
20. Liu L, Trimarchi JR, Smith PJ, Keete DL. Mitochondrial dysfunction leads to telomere attrition and genomic instability. Aging Cell. 2002; 1:40–46. [PubMed: 12882352]
21. Kurz DJ, Decary S, Hong Y, Trivier E, Akhmedov A, Erusalimsky JD. Chronic oxidative stress comprises telomere integrity and accelerates the onset of senescence in human endothelial cells. J Cell Sci. 2004; 117:2417–2426. [PubMed: 15126641]
22. Passos JF, von Zglinicki T. Mitochondria, telomeres and cell senescence. Exp Gerontol. 2005; 40:466–472. [PubMed: 15963673]
23. Richter T, Proctor C. The role of intracellular peroxide levels on the development and maintenance of telomere-dependent senescence. Exp Gerontol. 2007; 42:1043–1052. [PubMed: 17888604]
24. Voghel G, Thorin-Trescases N, Mamarbachi AM, Villeneaue L, Malette FA, Farbeyre G, Farhat N, Perrault LP, Carrier M, Therin E. Endogenous oxidative stress prevents telomerase-dependent immortalization of human endothelial cells. Mech Ageing Dev. 2010; 131:354–363. [PubMed: 20399802]

25. Doonan R, McElwee JJ, Matthijssens F, Walker GA, Houthoofd K, Back P, Matscheski A, Vanfleteren JR, Gems D. Against the oxidative damage theory of aging: Superoxide dismutases protect against oxidative stress but have little or no effect on life span in Caenorhabditis elegans. Genes Dev. 2008; 22:3236–3241. [PubMed: 19056880]
26. Gems D, Doonan R. Antioxidant defense and aging in C. elegans: Is the oxidative damage theory of aging wrong? Cell Cycle. 2009; 8:1681–1687. [PubMed: 19411855]
27. Blagosklonny MV. Program-like aging and mitochondria: Instead of random damage by free radicals. J Cell Biochem. 2007; 102:1389–1399. [PubMed: 17975792]
28. Blagosklonny MV. Aging: ROS or TOR. Cell Cycle. 2008; 7:3344–3354. [PubMed: 18971624]
29. Blagosklonny MV. Revisiting the antagonistic pleiotropy theory of aging: TOR-driven program and quasi-program. Cell Cycle. 2010; 9:3151–3156. [PubMed: 20724817]
30. Cabreiro F, Ackerman D, Doonan R, Araiz C, Back P, Papp D, Braeckman BP, Gems D. Increased life span from overexpression of superoxide dismutase in Caenorhabditis elegans is not caused by decreased oxidative damage. Free Radic Biol Med. 2011; 51:1575–1582. [PubMed: 21839827]
31. Lapointe J, Hekimi S. When a theory of aging ages badly. Cell Mol Life Sci. 2009; 67:1–8. [PubMed: 19730800]
32. Speakman JR, Selman C. The free-radical damage theory: Accumulating evidence against a simple link of oxidative stress to ageing and lifespan. Bioessays. 2011; 33:255–259. [PubMed: 21290398]
33. Blagosklonny MV. Damage-induced aging and perpetual motion. Cell Cycle. 2013; 12:2709–2710. [PubMed: 23966155]
34. Cohen LS, Studzinski GP. Correlation between cell enlargement and nucleic acid and protein content of HeLa cells in unbalanced growth produced by inhibitors of DNA synthesis. J Cell Physiol. 1967; 69:331–339. [PubMed: 4230858]
35. Traganos F, Darzynkiewicz Z, Melamed MR. The ratio of RNA to total nucleic acid content as a quantitative measure of unbalanced cell growth. Cytometry. 1982; 2:212–218. [PubMed: 6173180]
36. Burhans WC, Weinberger M. DNA replication stress, genome instability and aging. Nucleic Acids Res. 2007; 33:7545–7556. [PubMed: 18055498]
37. Hay N, Sonenberg N. Upstream and downstream of mTOR. Genes Dev. 2004; 18:1926–1945. [PubMed: 15314020]
38. Wullschleger S, Loewith R, Hall MN. TOR signaling in growth and metabolism. Cell. 2006; 124:471–484. [PubMed: 16469695]
39. Zoncu R, Efeyan A, Sabatini DM. mTOR: From growth signal integration to cancer, diabetes and ageing. Nat Rev Mol Cell Biol. 2010; 12:21–35. [PubMed: 21157483]
40. Ma XM, Blenis J. Molecular mechanisms of mTOR-mediated translational control. Nat Rev Mol Cell Biol. 2009; 10:307–318. [PubMed: 19339977]
41. Magnuson B, Ekim B, Fingar DC. Regulation and function of ribosomal protein S6 kinase (S6K) within mTOR signaling networks. Biochem J. 2012; 441:1–21. [PubMed: 22168436]
42. Blagosklonny MV, Hall MN. Growth and aging: A common molecular mechanism. Aging (Albany). 2009; 1:357–362.
43. Loewith R, Hall MN. Target of rapamycin (TOR) in nutrient signaling and growth control. Genetics. 2011; 189:1177–1201. [PubMed: 22174183]
44. Martin-Montalvo A, Mercken EM, Mitchell SJ, Palacios HH, Mote PL, Scheibye-Knudsen M, Gomes AP, Ward TM, Minor RK, Blouin MJ, et al. Metformin improves healthspan and lifespan in mice. Nature Commun. 2013; 4:2192. [PubMed: 23900241]
45. Cabreiro F, Au C, Leung KY, Vergara-Irigaray N, Cocheme HM, Noori T, Weinkove D, Schuster E, Greene ND, Gems D. Metformin retards aging in C. elegans by altering microbial folate and methionine metabolism. Cell. 2013; 153:228–239. [PubMed: 23540700]
46. Onken B, Driscoll M. Metformin induces a dietary restriction-like state and the oxidative stress response to extend *C. elegans* healthspan via AMPK, LKB1, and SKN-1. PLoS ONE. 2010; 5:e8758. [PubMed: 20090912]
47. Anisimov VN, Piskunova TS, Popovich IG, Zabezhinski MA, Tyndyk ML, Egormin PA, Yurova MV, Rosenfeld SV, Semenchenko AV, Kovalenko IG, et al. Gender differences in metformin

effect on aging, life span and spontaneous tumorigenesis in 129/ Sv mice. Aging (Albany). 2010; 2:945–958.

48. Anisimov VN. Metformin for aging and cancer prevention. Aging (Albany). 2010; 2:760–774.
49. Anisimov VN, Berstein LM, Popovich IG, Zabezhinski MA, Egormin PA, Piskunova TS, Semenchenko AV, Tyndyk ML, Yurova MN, Kovalenko IG, et al. If started early in life, metformin treatment increases life span and postpones tumors in female SHR mice. Aging (Albany NY). 2011; 3:148–157. [PubMed: 21386129]
50. Harrison DE, Strong R, Sharp ZD, Nelson JF, Astle CM, Flurkey K, Nadon NL, Wilkinson JE, Frenkel K, Carter CS, et al. Rapamycin fed late in life extends lifespan in genetically heterogeneous mice. Nature. 2009; 460:392–395. [PubMed: 19587680]
51. Wilkinson E, Burmeister L, Brooks SV, Chan CC, Friedline S, Harrison DE, Hejtmancik JF, Nadon N, Strong R, Wood LK, et al. Rapamycin slows aging in mice. Aging Cell. 2012; 11:675–682. [PubMed: 22587563]
52. Neff F, Flores-Dominguez D, Ryan DP, Horsch M, Schroder S, Adler T, Afonso LC, Aguilar-Pimentel JA, Becker L, Garrett L, et al. Rapamycin extends murine lifespan but has limited effects on aging. J Clin Invest. 2013; 123:3272–3291. [PubMed: 23863708]
53. Ma TC, Buescher JL, Oatis B, Funk JA, Nash AJ, Carrier RL, Hoyt KR. Metformin therapy in a transgenic mouse model of Huntington's disease Neurosci Lett. 2007; 411:98–103.
54. Anisimov VN, Bartke A. The key role of growth hormone-insulin- GF-1 signaling in aging and cancer. Crit Rev Oncol Hematol. 2013; 87:201–223. [PubMed: 23434537]
55. Bartke A. Growth hormone, insulin and aging: The benefits of endocrine defects. Exp Gerontol. 2011; 46:108–111. [PubMed: 20851173]
56. Barzilai N, Huffman DM, Muzumdar RH, Bartke A. The critical role of metabolic pathways in aging. Diabetes. 2012; 61:1315–1322. [PubMed: 22618766]
57. Bartke A. Single-gene mutations and healthy ageing in mammals. Philos Trans R Soc Lond B Biol Sci. 2011; 366:28–34. [PubMed: 21115527]
58. Bartke A, Brown-Borg H. Life extension in the dwarf mouse. Curr Top Dev Biol. 2004; 63:189–225. [PubMed: 15536017]
59. Stout GJ, Stigter EC, Essers PB, Mulder KW, Kolkman A, Snijders DS, van den Broek NJ, Betist MC, Korswagen HC, Macinnes AW, et al. Insulin/IGF-1-medi-ated longevity is marked by reduced protein metabolism. Mol Syst Biol. 2013; 9:679. [PubMed: 23820781]
60. Ruan JW, Liao YC, Lua I, Li MH, Hsu CY, Chen JH. Human pituitary tumor-transforming gene 1 overexpression reinforces oncogene-induced senescence through CXCR2/p21 signaling in breast cancer cells. Breast Cancer Res. 2012; 14:R106. [PubMed: 22789011]
61. Lamming DW, Ye L, Sabatini DM, Baur JA. Rapalogs and mTOR inhibitors as anti-aging therapeutics. J Clin Invest. 2013; 123:980–989. [PubMed: 23454761]
62. Blagosklonny MV. Rapamycin extends life- and health span because it slows aging. Aging (Albany NY). 2013
63. Komarova EA, Antoch MP, Novototskaya LR, Chernova OB, Paszkiewicz G, Leontieva OV, Blagosklonny MV, Gudkov AV. Rapamycin extends lifespan and delays tumorigenesis in heterozygous p53+/− mice. Aging (Albany NY). 2012; 4:709–714. [PubMed: 23123616]
64. Blagosklonny MV. Increasing healthy lifespan by suppressing aging in our lifetime: Preliminary proposal. Cell Cycle. 2010; 9:4788–4794. [PubMed: 21150328]
65. Anisimov VN. Metformin: Do we finally have an anti-aging drug? Cell Cycle. 2013; 12:3483–4389. [PubMed: 24189526]
66. Wang Q, Zhang M, Liang B, Shirwany N, Zhu Y, Zou MH. Activation of AMP activated protein kinase is required for berberine-induced reduction of artheriosclerosis in mice: The role of uncoupling protein 2. PLoS One. 2011:e25436. [PubMed: 21980456]
67. Li H, Miyahara T, Tezuka Y, Tran OL, Seto H, Kadota S. Effect of berberine on bone mineral density in SAMP6 as a senile osteoporosis model. Biol Pharma Bull. 2003; 26:130–131.
68. Ki HF, Shen L. Berberine: A potential multipotent natural product to combat Alzheimer's Disease. Molecules. 2011; 16:6732–6740. [PubMed: 21829148]

69. Cicero AF, Tartagani E. Antidiabetic properties of berberine: From cellular pharmacology to clinical effects. Hosp Pract (Minneap). 2012; 40:56–63.
70. Shen N, Huan Y, Shen ZF. Berberine inhibits mouse insulin gene promoter through activation of AMP activated protein kinase and may exert beneficial effect on pancreatic β-cell. Eur J Pharmacol. 2012:S0014–S2099. 00697-8.
71. Derosa G, Maffioli P, Cicero AF. Berberine on metabolic and cardiovascular risk factors: An analysis from preclinical evidences to clinical trials. Expert Opin Biol Ther. 2012; 12:1113–1124. [PubMed: 22780092]
72. Halicka HD, Zhao H, Li J, Lee Y-S, Hsieh T-C, Wu JM, Darzynkiewicz Z. Potential anti-aging agents suppress the level of constitutive DNA damage- and mTOR- signaling. Aging (Albany). 2012; 4:952–965.
73. Zhao H, Halicka HD, Li J, Darzynkiewicz Z. Berberine suppresses gero-conversion from cell cycle arrest to senescence. Aging (Albany). 2013; 6:633–636.
74. Dieterlen MT, Bittner HB, Klein S, von Salisch S, Mittag A, Tarnok A, Dhein S, Mohr FW, Barten MJ. Assay validation of phosphorylated S6 ribosomal protein for a pharmacodynamic monitoring of mTOR-inhibitors in peripheral human blood. Cytometry B Clin Cytom. 2012; 82:151–157. [PubMed: 22213594]
75. Sigrist SJ, Carmona-Gutierrez D, Gupta VK, Bhukel A, Mertel S, Eisenberg T, Madeo F. Spermidine-triggered autophagy ameliorates memory during aging. Autophagy. 2014; 10:178–179. [PubMed: 24262970]
76. Pyo JO, Yoo SM, Jung YK. The interplay between autophagy and aging. Diabetes Metab J. 2013; 37:333–339. [PubMed: 24199161]
77. Gelino S, Hansen M. Autophagy—an emerging anti-aging mechanism. J Clin Exp Pathol. 2012; (Suppl 4.pii):006. [PubMed: 23750326]
78. Morselli E, Galluzzi L, Kepp O, Criollo A, Maiuri MC, Tavernarakis N, Madeo F, Kroemer G. Autophagy mediates pharmacological lifespan extension by spermidine and resveratrol. Aging (Albany). 2009; 1:961–970.
79. Morselli E, Maiuri MC, Markaki M, Megalou E, Pasparaki E, Palikaras K, Criollo A, Galluzzi L, Malik SA, Vitale I, Michaud M, Madeo F, Tavernarakis N, Kroemer G. Caloric restriction and resveratrol promote longevity through the Sirtuin-1-dependent induction of autophagy Cell Death and Disease. 2010:e10.
80. Yamaguchi O, Otsu K. Role of autophagy in aging. J Cardiovasc Pharmacol. 2012; 60:242–247. [PubMed: 22343371]
81. Rubinsztein DC, Marino G, Kroemer G. Autophagy and aging. Cell. 2011; 148:682–695. [PubMed: 21884931]
82. Sauve AA, Wolberger C, Schramm BVL, Boeke JD. The biochemistry of sirtuins. Annu Rev Biochem. 2006; 75:435–465. [PubMed: 16756498]
83. Minois N, Carmona-Gutierrez D, Madeo F. Polyamines in aging and disease. Aging (Albany). 2011; 3:716–732.
84. Miller RA, Harrison DE, Astle CM, Baur JA, Boyd AR, de Cabo R, Fernandez E, Flurkey K, Javors MA, Nelson JF, et al. Rapamycin, but not resveratrol or simvastatin, extends life span of genetically heterogeneous mice. J. Gerontol. A Biol Sci Med Sci. 2011; 66:191–201. [PubMed: 20974732]
85. Thapa D, Ghosh R. Antioxidants for prostate cancer chemoprevention: Challenges and opportunities. Biochem Pharmacol. 2012; 83:1319–1330. [PubMed: 22248733]
86. Blagosklonny MV. Hypoxia, mTOR and autophagy: Converging on senescence or quiescence. Autophagy. 2013; 9:260–262. [PubMed: 23192222]
87. Li D. Metformin as an antitumor agent in cancer prevention and treatment. J Diabetes. 2011; 3:320–327. [PubMed: 21631893]
88. Buitrago-Molina LE, Vogel A. mTOR as a potential target for the prevention and tratment of hepatocellular carcinoma. Curr Cancer Drug Target. 2012; 12:1045–1061.
89. Blagosklonny MV. Rapalogs in cancer prevention: Anti-aging or anticancer? Cancer Biol Ther. 2012; 13:1349–1354. [PubMed: 23151465]

90. Lopez-Torres M, Gredilla , Alberto Sanz A, Barja G. Influence of aging and long-term caloric restriction on oxygen radical generation and oxidative DNA damage in rat liver mitochondria. Free Radic Biol Med. 2002; 32:882–889. [PubMed: 11978489]
91. Tanaka T, Halicka HD, Huang X, Traganos F, Darzynkiewicz Z. Constitutive histone H2AX phosphorylation and ATM activation, the reporters of DNA damage by endogenous oxidants. Cell Cycle. 2006; 5:1940–1945. [PubMed: 16940754]
92. Zhao H, Tanaka T, Halicka HD, Traganos F, Zarebski M, Dobrucki J, Darzynkiewicz Z. Cytometric assessment of DNA damage by exogenous and endogenous oxidants reports the aging-related processes. Cytometry A. 2007; 71A:905–914. [PubMed: 17879239]
93. Huang X, Tanaka T, Kurose A, Traganos F, Darzynkiewicz Z. Constitutive histone H2AX phosphorylation on *Ser*-139 in cells untreated by genotoxic agents is cell-cycle phase specific and attenuated by scavenging reactive oxygen species. Int J Oncol. 2006; 29:495–501. [PubMed: 16820894]
94. Zhao H, Tanaka T, Mitlitski V, Heeter J, Balazs EA, Darzynkiewicz Z. Protective effect of hyaluronate on oxidative DNA damage in WI-38 and A549 cells. Int J Oncol. 2008; 32:1159–1169. [PubMed: 18497977]
95. Tanaka T, Kurose A, Halicka HD, Traganos F, Darzynkiewicz Z. 2-Deoxy-D-glucose reduces the level of constitutive activation of ATM and phosphorylation of histone H2AX. Cell Cycle. 2006; 5:878–882. [PubMed: 16628006]
96. Tanaka T, Kajstura M, Halicka HD, Traganos F, Darzynkiewicz Z. Constitutive histone H2AX phosphorylation and ATM activation are strongly amplified during mitogenic stimulation of lymphocytes. Cell Prolif. 2007; 40:1–13. [PubMed: 17227291]
97. Yang NC, Song TY, Chen MY, Hu ML. Effects of 2-deoxyglucose and dehydroepian-drosterone on intracellular NAD(+) level, SIRT1 activity and replicative lifespan of human Hs68 cells. Biogerontology. 2011; 12:527–536. [PubMed: 21604001]
98. Ingram DK, Roth GS. Glycolitic inhibition as a strategy for developing calorie restriction mimetics. Exp Gerontol. 2011; 46:148–154. [PubMed: 21167272]
99. Smith DL, Nagy TR, Allison DB. Calorie restriction: What recent results suggest for the future of ageing research. Eur J Clin Invest. 2010; 40:440–450. [PubMed: 20534066]
100. Diogo CV, Machado NG, Barbosa IA, Serafim TL, Burgeiro A, Oliveira PJ. Berberine a promising safe anti-cancer agent—is there a role for mitochondria? Curr Drug Targets. 2011; 12:850–859. [PubMed: 21269266]
101. Wang Q, Zhang M, Liang B, Shirwany N, Zhu Y, Zou MH. Activation of AMP-activated protein kinase is required for berberine-induced reduction of artheriosclerosis in mice: The role of uncoupling protein 2. PLoS One. 2011:e25436. [PubMed: 21980456]
102. Li H, Miyahara T, Tezuka Y, Tran OL, Seto H, Kadota S. Effect of berberine on bone mineral density in SAMP6 as a senile osteoporosis model. Biol Pharma Bull. 2003; 26:130–131.
103. Ki HF, Shen L. Berberine: A potential multipotent natural product to combat Alzheimer's Disease. Molecules. 2011; 16:6732–6740. [PubMed: 21829148]
104. Shen N, Huan Y, Shen ZF. Berberine inhibits mouse insulin gene promoter through activation of AMP activated protein kinase and may exert beneficial effect on pancreatic β-cell. Eur J Pharmacol. 2012; 694:120–126. [PubMed: 22955013]
105. Klotz B, Mentrup B, Regensburger M, Zeck S, Schneidereit J, Schupp N, Linded C, Merz C, Ebert R, Jakob F. 1,25-Dihydroxyvitamin D3 treatment delays cellular aging in human mesenchymal stem cells while maintaining their multipotent capacity. PLoS One. 2012; 7:e29959. [PubMed: 22242193]
106. Haussler MR, Haussler CA, Whitfield GK, Hsieh JC, Thompson PD, Barthel TK, Bartik L, Egan JB, Wu Y, Kubicek JL, et al. The nuclear vitamin D receptor controls the expression of genes encoding factors which feed the "Fountain of Youth" to mediate healthful Aging. J Steroid Biochem Mol Biol. 2010; 121:88–97. [PubMed: 20227497]
107. Touhimm P. Vitamin D and aging. J Steroid Biochem Mol Biol. 2009; 114:78–84. [PubMed: 19444937]
108. Lanske B, Razzaque MS. Vitamin D and aging: Old concepts and new insights. J Nutr Biochem. 2007; 18:771–777. [PubMed: 17531460]

109. Forster RE, Jurutka PW, Hsieh JC, Haussler CA, Lowmiller CL, Kaneko I, Haussler MR, Kerr WH. Vitamin D receptor controls expression of the anti-aging klotho gene in mouse and human renal cells. Biochem Biophys Res Commun. 2011; 414:557–562. [PubMed: 21982773]
110. Vetterli L, Maechler P. Resveratrol-activated SIRT1 in liver and pancreatic β-cells: A Janus head looking to the same direction of metabolic homeostasis. Aging (Albany). 2011; 3:444–449.
111. Gerhardt E, Graber S, Szego EM, Moisol N, Martins LM, Outeiro TF, Kermer P. Idebebone and resveratrol extend life span and improve motor function of HtrA2 knockout mice. PLoS One. 2011; 6:e28855. [PubMed: 22205977]
112. Rascon B, Hubbard BP, Sinclair DA, Amdam GV. The lifespan extension effects of resveratrol are conserved in the honey bee and may be driven by a mechanism related to caloric restriction. Aging (Albany). 2012; 4:499–508.
113. Chung JH, Manganiello V, Dyck JR. Resveratrol as a calorie restriction mimetic: Therapeutic implications. Trends Cell Biol. 2012; 22:546–554. [PubMed: 22885100]
114. Timmers S, Auwerx J, Schrauwen P. The journey of resveratrol from yeast to human. Aging (Albany). 2012; 4:146–158.
115. Bass TM, Weinkove G, Hourthoofd K, Gems D, Partridge L. Effects of resveratrol on lifespan in Drosophila melanogaster and Caenorhabditis elegans. Mech Ageing Dev. 2007; 128:546–552. [PubMed: 17875315]
116. Ayyadevara S, Bharill P, Dandapat A, Hu C, Khaidakov M, Mitra S, Shmookler Reis RJ, Mehta JL. Aspirin inhibits oxidant stress, reduces age-associated functional declines, and extends lifespan of caenorhabditis elegans. Antioxid Redox Signal. 2013; 18:481–490. [PubMed: 22866967]
117. Bode-Boger SM, Martens-Lobenhoffer J, Tager M, Schroder H, Scalera F. Aspirin reduces endothelial cell senescence. Biochem Biophys Res Commun. 2005; 334:1226–1232. [PubMed: 16039999]
118. Strong B, Miller RA, Astie CM, Floyd RA, Flurkey K, Hensley KL, Javors MA, Leeuwenburgh C, Nelson JF, Ongini E, Nadon NL, Warner HR, Harrison DE. Nordihydroguaiaretic acid and aspirin increase lifespan of genetically heterogenous male mice. Aging Cell. 2008; 7:641–650. [PubMed: 18631321]
119. Yi TN, Zhao HY, Zhang JS, Shan HY, Meng X, Zhang J. Effect of aspirin on high glucose-induced senescence of endothelial cells. Chin Med J (Engl). 2009; 20(122):3055–3061. [PubMed: 20137501]
120. Mcllhatton MA, Tyler J, Kerepesi LA, Bocker-Edmonston T, Kucherlapati MH, Edelmann W, Kucherlapati R, Kopelovich L, Fishel L. Aspirin and low-dose nitricoxide-donating aspirin increase life span in a Lynch syndrome mouse model. Cancer Prev Res (Phila). 2011; 4:684–693. [PubMed: 21436383]
121. Bulckaen H, Prevost G, Boulanger E, Robitaille G, Roquet V, Gaxatte C, Garcon G, Corman B, Gosset P, Shirali P, et al. Low-dose aspirin prevents age-related endothelial dysfunction in a mouse model of physiological aging. Am J Physiol Heart Circ Physiol. 2008; 294:H1562–H1570. [PubMed: 18223195]
122. Halicka HD, Zhao H, Li J, Traganos F, Zhang S, Lee M, Darzynkiewicz Z. Genome protective effect of metformin as revealed by reduced level of constitutive DNA damage signaling. Aging (Albany). 2011; 3:1028–1038.
123. Halicka HD, Zhao H, Li J, Traganos DF, Studzinski G, Darzynkiewicz Z. Attenuation of constitutive DNA damage signaling by 1,25-dihydroxyvitamin D3. Aging (Albany). 2012; 4:270–278.
124. Halicka HD, Ita M, Tanaka T, Kurose A, Darzynkiewicz Z. The biscoclaurine alkaloid cepharanthine protects DNA in TK6 lymphoblastoid cells from constitutive oxidative damage. Pharmacol Rep. 2008; 60:93–100. [PubMed: 18276990]
125. Robinson JP. Oxidative metabolism. Curr Protoc Cytom. 2001; Chapter 9(Unit 9.7)
126. Darzynkiewicz Z, Traganos F, Staiano-Coico L, Kapuscinski J, Melamed MR. Interactions of rhodamine 123 with living cells studied by flow cytometry. Cancer Res. 1982; 42:799–806. [PubMed: 7059978]

127. Darzynkiewicz Z, Staiano-Coico L, Melamed MR. Increased mitochondrial uptake of rhodamine 123 during lymphocyte stimulation. Proc Natl Acad Sci USA. 1981; 78:2383–2387. [PubMed: 6941298]
128. Pozarowski P, Holden E, Darzynkiewicz Z. Laser scanning cytometry: Principles and applications. An update. Methods Mol Biol. 2013; 913:187–212. [PubMed: 23027005]
129. Juan G, Gruenwald S, Darzynkiewicz Z. Phosphorylation of retinoblastoma susceptibility gene protein assayed in individual lymphocytes during their mitogenic stimulation. Exp Cell Res. 1998; 239:104–110. [PubMed: 9511729]
130. Juan G, Gruenwald S, Darzynkiewicz Z. Flow cytometric methods for the concurrent detection of discrete functional conformations of pRB in single cells. US patent. Nov 23.2004 No. 6(821): 740.
131. Dimri GP, Lee X, Basile G, Acosta M, Scott G, Rockelley C, Medrano EE, Linskens M, Rubelj I, Pereira-Smith O, Peacocke M, Campisi J. A biomarker that identifies senescent human cells in culture and in aging skin in vivo. Proc Natl Acad Sci USA. 1995; 92:9363–9367. [PubMed: 7568133]
132. Zhao H, Halicka HD, Jorgensen E, Traganos F, Darzynkiewicz Z. New biomarkers probing the depth of cell senescence assessed by laser scanning cytometry. Cytometry A. 2010; 77A:999–1007. [PubMed: 20939035]
133. Zhao H, Darzynkiewicz Z. Biomarkers of cell senescence assessed by imaging cytometry. Methods Mol Biol. 2013; 965:83–92. [PubMed: 23296652]
134. McKenna E, Traganos F, Zhao H, Darzynkiewicz Z. Persistent DNA damage caused by low levels of mitomycin C induces irreversible senescence of A549 cells. Cell Cycle. 2012; 12:3132–3140. [PubMed: 22871735]
135. Pospelova TV, Chitikova ZV, Pospelov VA. An integrated approach for monitoring cell senescence. Methods Mol Biol. 2013; 965:383–408. [PubMed: 23296673]
136. Cho S, Park J, Hwang ES. Kinetics of the cell biological changes occurring in the progression of DNA damage-induced senescence. Mol Cells. 2011; 31:539–546. [PubMed: 21533552]
137. Perillo NL, Naeim F, Walford RL, Effros RB. In vitro cellular aging in T-lymphocyte cultures: Analysis of DNA content and cell size. Exp Cell Res. 1993; 207:131–135. [PubMed: 8319764]
138. Ormerod MG, Paul F, Cheetham M, Sun XM. Discrimination of apoptotic thymocytes by forward light scatter. Cytometry A. 2005; 21A:300–305.
139. Darzynkiewicz Z, Bruno S, Del Bino G, Gorczyca W, Hotz MA, Lassota P, Traganos F. Features of apoptotic cells measured by flow cytometry. Cytometry. 1992; 13:795–808. [PubMed: 1333943]
140. Patel KV, Ferruci L, Ershler WB, Longo DL, Guralnik JM. Red cell distribution width and the risk of death in middle-aged and older adults. Arch Intern Med. 2009; 169:515–523. [PubMed: 19273783]
141. Philipps AF, Persson B, Hall K, Lake M, Skottner A, Sanengen T, Sara VR. The effects of biosynthetic insulin-like growth factor-1 supplementation on somatic growth, maturation, and erythropoiesis on the neonatal rat. Pediatr Res. 1988; 23:298–305. [PubMed: 3353177]
142. Kurtz A, Jelkmann W, Bauer C. A new candidate for the regulation of erythropoiesis: Insulin-like growth factor I. FEBS Lett. 1982; 22:105–108. [PubMed: 6759171]
143. Kim I, Kim CH, Yim YS, Ahn YS. Autocrine function of erythropoietin in IGF-1-induced erythropoietin biosynthesis. Neuroreport. 2008; 9:1699–1703. [PubMed: 18841090]
144. Kling PJ, Taing KM, Dvorak B, Woodward SS, Philipps AF. Insulin-like growth factor-I stimulates erythropoiesis when administered enterally. Growth Factors. 2006; 24:218–223. [PubMed: 17079205]
145. Ratajczak J, Zhang Q, Pertusini E, Wojczyk BS, Wasik MA, Ratajczak MZ. The role of insulin (INS) and insulin-like growth factor-1 (IGF-I) in regulating human erythropoiesis Studies in vitro under serum-free conditions—comparison to other cytokines and growth factors. Leukemia. 1998; 12:371–381. [PubMed: 9529132]
146. Sun H, Tu X, Baserga R. A mechanism for cell size regulation by the insulin and insulin-like growth factor-1 receptors. Cancer Res. 2006; 66:11106–11109. [PubMed: 17145851]

147. Kozlitina J, Garcia CK. Red blood cell size is inversely associated with leukocyte telomere length in a large multi-ethnic population. PLoS One. 2012; 7:e51046. [PubMed: 23226558]

148. Movérare-Skrtic S, Svensson J, Karlsson MK, Orwoll E, Ljunggren O, Mellström D, Ohlsson C. Serum insulin-like growth factor-I concentration is associated with leukocyte telomere length in a population-based cohort of elderly men. J Clin Endocrinol Metab. 2009; 94:5078–5084. [PubMed: 19846733]

149. Barbieri M, Paolisso G, Kimura M, Gardner JP, Boccardi V, Papa M, Hjelmborg JV, Christensen K, Brimacombe M, Nawrot TS, et al. Higher circulating levels of IGF-1 are associated with longer leukocyte telomere length in healthy subjects. Mech Ageing Dev. 2009; 130:771–776. [PubMed: 19913048]

150. Aubert G, Hills M, Lansdorp PM. Telomere length measurement-caveats and a critical assessment of the available technologies and tools. Mutat Res. 2012; 730:59–67. [PubMed: 21663926]

151. Baerlocher GM, Vulto I, de Jong G, Lansdorp PM. Flow cytometry and FISH to measure the average length of telomeres (flow FISH). Nat Protoc. 2006; 1:2365–2376. [PubMed: 17406480]

152. Schmid I, Jamieson BD. Assessment of telomere length, phenotype, and DNA content. Curr Protoc Cytom. 2004; Chapter 7(Unit 7.26)

153. Tzanetakou IP, Nzietchueng R, Perrea DN, Benetos A. Telomeres and their role in aging and longevity. Curr Vasc Pharmacol. 2013 Dec 18. [Epub].

154. Takubo K, Aida J, Izumiyama-Shimomura N, Ishikawa N, Sawabe M, Kurabayashi R, Shiraishi H, Arai T, Nakamura K. Changes of telomere length with aging. Geriatr Gerontol Int. 2010; (Suppl 1):S197–S206. [PubMed: 20590834]

155. Zekry D, Krause KH, Irminger-Finger I, Graf CE, Genet C, Vitale AM, Michel JP, Gold G, Herrmann FR. Telomere length, comorbidity, functional, nutritional and cognitive status as predictors of 5 years post hospital discharge survival in the oldest old. Nutr Health Aging. 2012; 16:225–230.

156. Barrett EL, Richardson DS. Sex differences in telomeres and lifespan. Aging Cell. 2011; 10:913–921. [PubMed: 21902801]

157. Macieira-Coelho A. Cell division and aging of the organism. Biogerontology. 2011; 12:503–515. [PubMed: 21732041]

158. Traganos F, Darzynkiewicz Z. Lysosomal proton pump activity: Supravital cell staining with acridine orange differentiates leukocyte subpopulations. Methods Cell Biol. 1994; 41:185–194. [PubMed: 7532261]

159. Lee JS, Lee GM. Monitoring of autophagy in Chinese hamster ovary cells using flow cytometry. Methods. 2012; 56:375–382. [PubMed: 22142658]

160. Chen Y, Azad MB, Gibson SB. Methods for detecting autophagy and determining autophagy-induced cell death. Can J Physiol Pharmacol. 2010; 88:285–295. [PubMed: 20393593]

161. Barth S, Glick D, Macleod KF. Autophagy: Assays and artifacts. J Pathol. 2010; 221:117–124. [PubMed: 20225337]

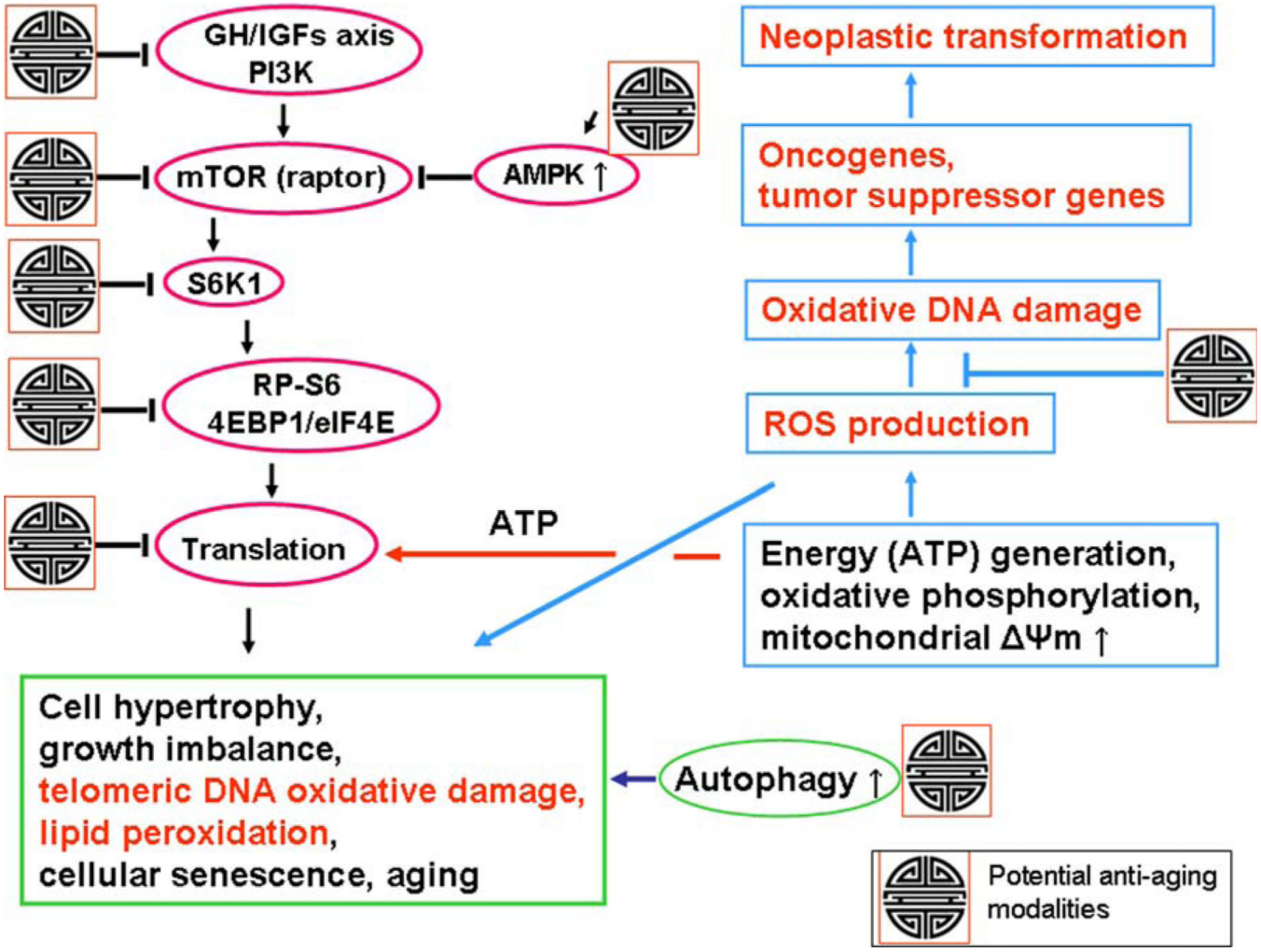

Figure 1.

Schematic presentation of the key pathways associated with cellular senescence and aging linking mTOR- and DNA damage-signaling as well as marking of sites for potential antiaging intervention. Signaling from several upstream pathways activated by insulin, IGFs, growth hormone (GH), or amino acids converges on, and activates, mTOR (raptor). mTOR stimulation triggers activation of S6K1 that results in phoshorylation of RP-S6 and 4EBP1, the factors indicative of activation of initiation and continuation of translation, This leads to cell growth, and particularly when cell division is postponed (e.g., because of replication stress), to growth imbalance (hypertrophy) characterized by the increased ratio of protein and RNA to DNA content, the hallmark of cellular senescence. As translation requires constant generation of energy (ATP), the oxidative phosphorylation in mitochondria persistently produces ROS. mTOR stimulation, thus, is inherently associated with generation of ROS. The oxidative DNA damage caused by endogenous ROS, when it occurs in sites coding for oncogenes or tumor suppressor genes, may lead to neoplasic transformation. Oxidative DNA damage of the telomeric DNA may cause telomere dysfunction and lead to replicative senescence, while lipid peroxidation is also a gero-promoting event, one of the typical features of the cellular senescence phenotype. The potential targets for antiaging

modalities are marked with the Chinese symbol of longevity (see the text). One of the most attractive targets is AMPK whose activation inhibits mTOR signaling. Among AMPK activators that show gero-suppressive properties are metformin and berberine. The antioxidants, by scavenging ROS, have primarily chemopreventive properties but by preventing oxidative telomeric DNA damage and lipid per-oxidation they also attenuate the aging process. The gero-suppressive role of autophagy, which often is seen to be activated by inhibitors of mTOR, is also well recognized (86). [Color figure can be viewed in the online issue, which is available at wileyonlinelibrary.com.]

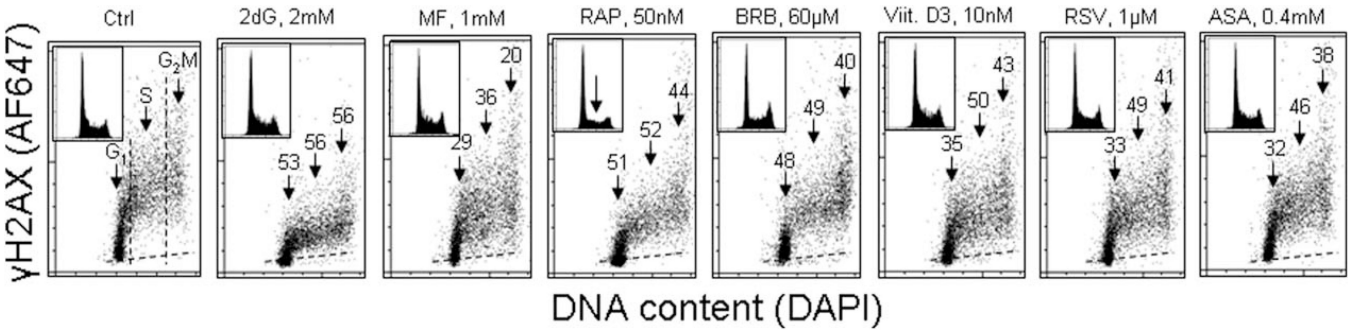

Figure 2.

Effect of exposure of TK6 cells to different reported antiaging drugs on the level of constitutive expression of γH2AX. Exponentially growing TK6 cells were untreated (Ctrl) or treated with the respective agents for 24 h at concentrations as shown. Expression of γH2AX in individual cells was detected immunocytochemically with the phospho-specific Ab (AlexaFluor647; AF647), DNA was stained with DAPI; cellular fluorescence was measured by flow cytometry as described (72). Cells were gated in the respective phases of the cell cycle based on differences in DNA content, as marked by the dashed vertical lines. The percent decrease in mean γH2AX fluorescence intensity of the treated cells in particular phases of the cell cycle, with respect to the respective untreated controls, is shown above the arrows. Inserts present DNA content frequency histograms from the individual cultures. The dashed skewed lines show the background level, the mean fluorescence intensity of the cells stained with secondary Ab only (72).

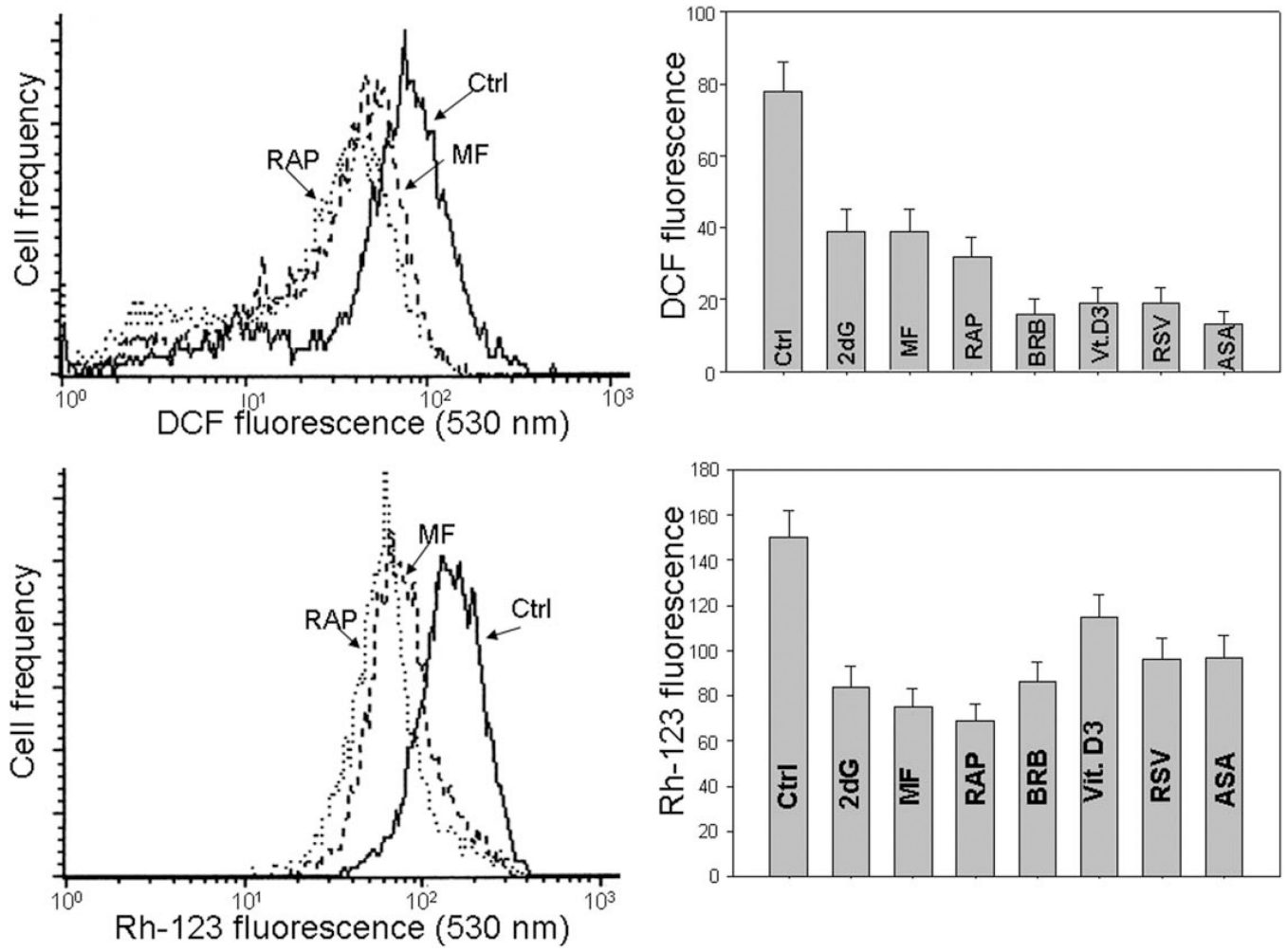

Figure 3.

The reduction of intracellular level of ROS measured by DCF fluorescence and of mitochondrial potential (ΔΨm) measured by rhodamine 123 (Rh-123) binding, by the reported gero-suppressive agents. Top panels: TK6 cells untreated (Ctrl) or treated for 24 h with the investigated agents, were exposed for 30 min to H_2DCF-DA and their fluorescence intensity was measured by flow cytometry (125). The cell-permeant nonfluorescent H_2DCF-DA upon cleavage of the acetate moiety by intercellular esterases and oxidation by ROS is converted to strongly fluorescent DCF and thus reports the ROS abundance. Left panel shows the frequency histograms of the untreated (Ctrl) as well MF- and RAP-treated cells (note exponential scale of the DCF fluorescence). Right panel presents the mean values (+SD) of DCF fluorescence of the untreated (Ctrl) and treated cells. Bottom panels: The cells were untreated (Ctrl) or treated as above then exposed for 30 min to the mitochondrial probe rhodamine 123 (Rh-123), and their fluorescence intensity was measured by flow cytometry (72). Left panel shows the frequency histograms of the untreated (Ctrl) as well MF- and RAP-treated cells (note exponential scale of the DCF fluorescence). Right panel presents the mean values (+SD) of Rh-123 fluorescence of the investigated cells (72,127).

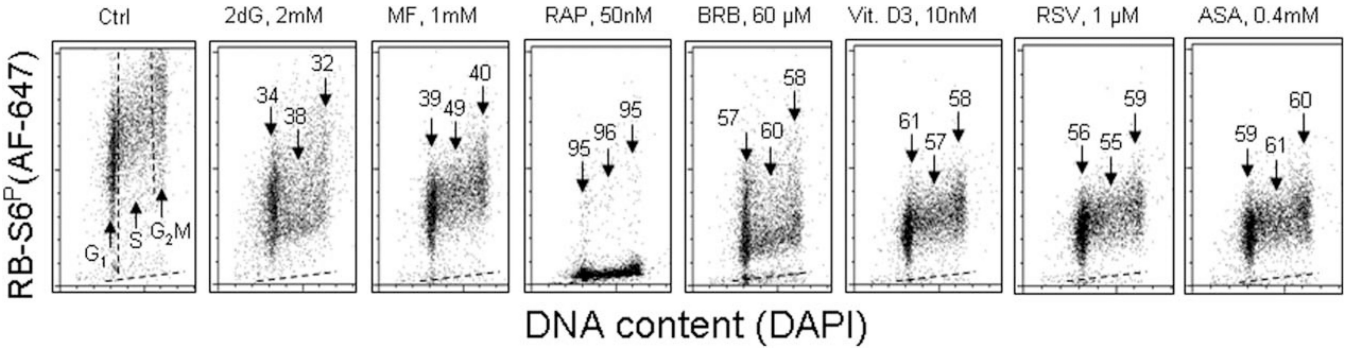

Figure 4.

The reduction of constitutive phosphorylation of ribosomal protein S6 (RP-S6) in TK6 cells treated with antiaging drugs. Exponentially growing TK6 cells were untreated (Ctrl) or treated with the respective agents at concentrations as shown, for 24 h. Based on differences in DNA content cells were gated in the respective phases of the cell cycle, as marked by the dashed vertical lines (Ctrl). The percent decrease in the RP-S6^P mean fluorescence intensity of the treated cells in particular phases of the cell cycle, with respect to the same phases of the untreated cells, is shown above the arrows. The dashed skewed lines show the background level, the mean fluorescence intensity of the cells stained with secondary Ab only.

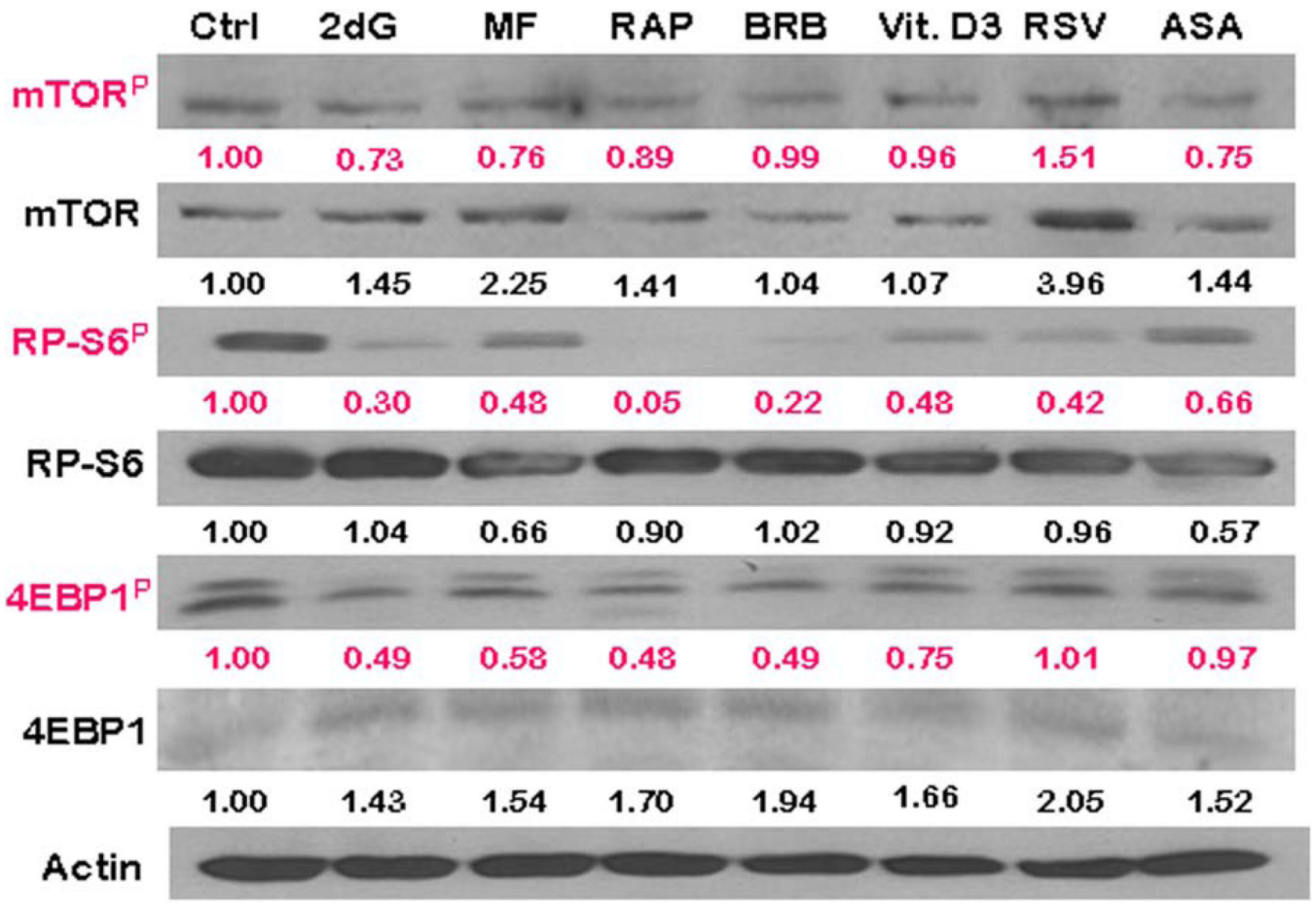

Figure 5.

The expression of mTOR-Ser2448^{P}, RP-S6-Ser235/236^{P}, and 4EBP1-Ser65^{P} and their respective total protein content, as detected by Western blotting. TK6 cells were exposed to the gero-suppressive agents at concentrations as shown in Figure 2 for 24 h. The protein expression was determined by Western blot analysis using either the phospho-specific (red) or total protein Abs (black) Abs and the intensity of the specific immuno-reactive bands were quantified by densitometry and normalized to actin (loading control). The numbers indicate the n-fold change in expression of the respective phospho-proteins in the drug-treated cultures with respect to the untreated cells (Ctrl). [Color figure can be viewed in the online issue, which is available at wileyonlinelibrary.com.]

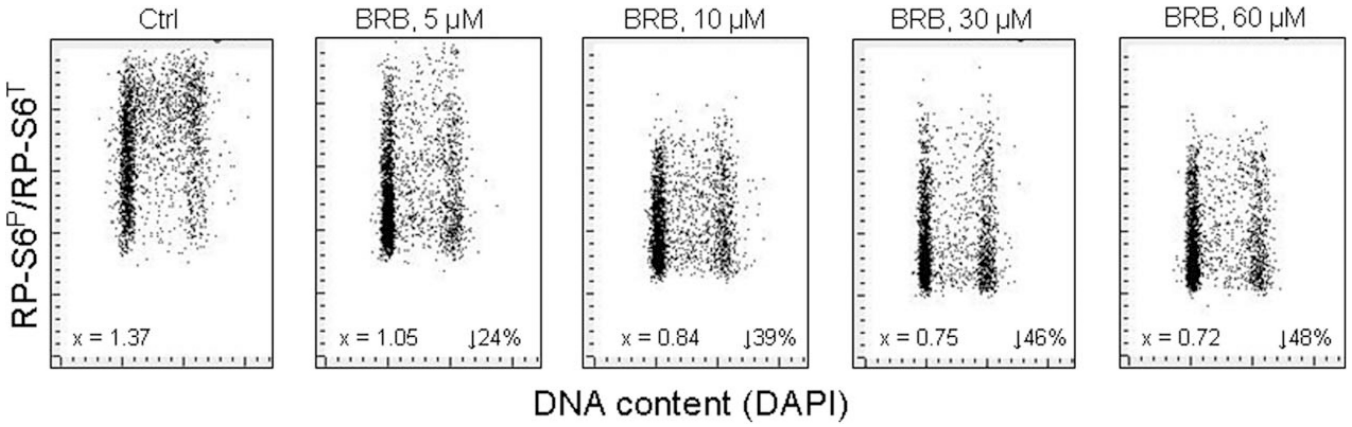

Figure 6.

Decreased ratio of phosphorylated RP-S6 (RP-$S6^P$) to total RP-S6 (RP-$S6^T$) in A549 cells treated with different concentration of BRB. A549 cells were untreated (Ctrl) or treated for 24 h with BRB at concentration as shown, RP-$S6^P$ was then detected using phospho-specific primary Ab and secondary Ab tagged with AlexaFluor 647 (AF647) while total RP-S6 (RP-$S6^T$) was detected using primary RP-S6 (not phospho-specific) Ab and secondary Ab AlexaFluor 488 (AF488), DNA was stained with DAPI. Intensity of cellular fluorescence was measured by laser scanning cytometry (LSC) and the ratiometric analysis of AF647/AF488 fluorescence intensities was carried out using the LSC software (128). The numbers on the left of the panels show the ratio of the mean values of integrated intensity of AF647 to AF488 fluorescence for all cells. The figures on right present the percent decrease of the ratio of BRB-treated cells vis-à-vis the Ctrl.

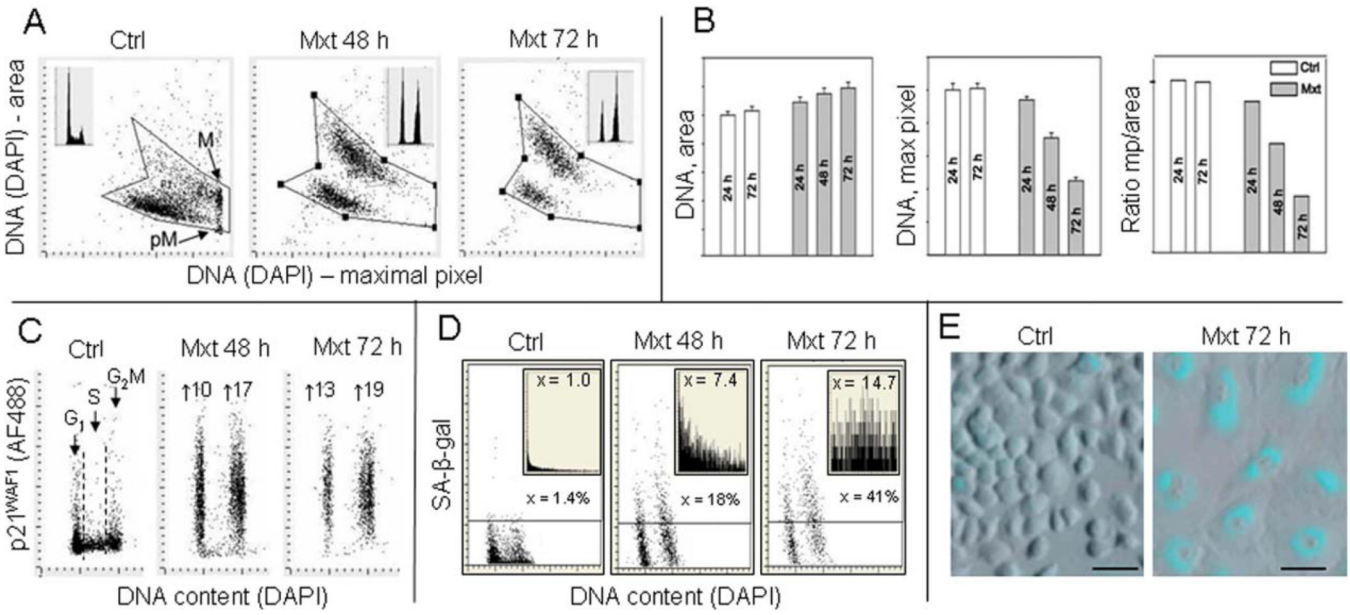

Figure 7.

Induction of premature cellular senescence of A549 cells measured by laser scanning cytometry. Human pulmonary lung adenocarcinoma A549 cells were untreated (Ctrl) or to induce cellular senescence were treated with 2-nM DNA topoisomerase II inhibitor mitoxantrone (Mxt) for 48 or 72 h. Panel **A** shows bivariate distributions of nuclear area versus intensity of maximal pixel of fluorescence revealed by measurement of nuclear DNA (DAPI) fluorescence. Intensity of maximal pixel is a marker of chromatin condensation and in the untreated cells has the highest value and marks mitotic (M) and immediately postmitotic (pM) G_1 cells, which also have low value of DAPI area. In the senescing cells, while nuclear area increases, the intensity of maximal pixel decreases (128,132–134). These morphometric changes reflect enlargement of the projected nuclear area and decreased DAPI local staining per unit area, due to flattened cellular appearance, the hallmark of cellular senescence (131–133). The insets show DNA content frequency histograms of cells from the respective cultures. Panel **B**: Bar plots reporting mean values (+SD) of nuclear (DNA, DAPI) area, DNA (DAPI) maximal pixel, and ratio of maximal pixel to nuclear area, respectively, of cells from control and Mxt treated cultures. Panel **C**: Bivariate distributions (DNA content vs p21) reporting expression of $p21^{WAF1}$ with respect to the cell cycle phase; the figures show the n-fold increase in mean expression of p21 of G_1 and G_2M cells from the Mxt-treated cultures with respect to respective cells in Ctrl. Panel **D**: Bivariate distributions of DNA content versus senescence-associated galactosidase (SA-β-gal) activity. Figures indicate percent of SA-β-gal positive (above the threshold marked by the horizontal lines) cells. Insets show the frequency distribution of SA-β-gal positive cells; the figures in insets show the n-fold increase in the mean activity of SA-β-gal in Mxt-treated cultures over Ctrl (1.0). Panel **E**: Images of cells growing in the absence (left) and presence of 2 nM Mxt for 72 h (right) stained to detect activation of SA-β-gal activity recorded by laser scanning cytometer (Research Imaging Cytometer iCys); 50 μm bars mark the length scale.

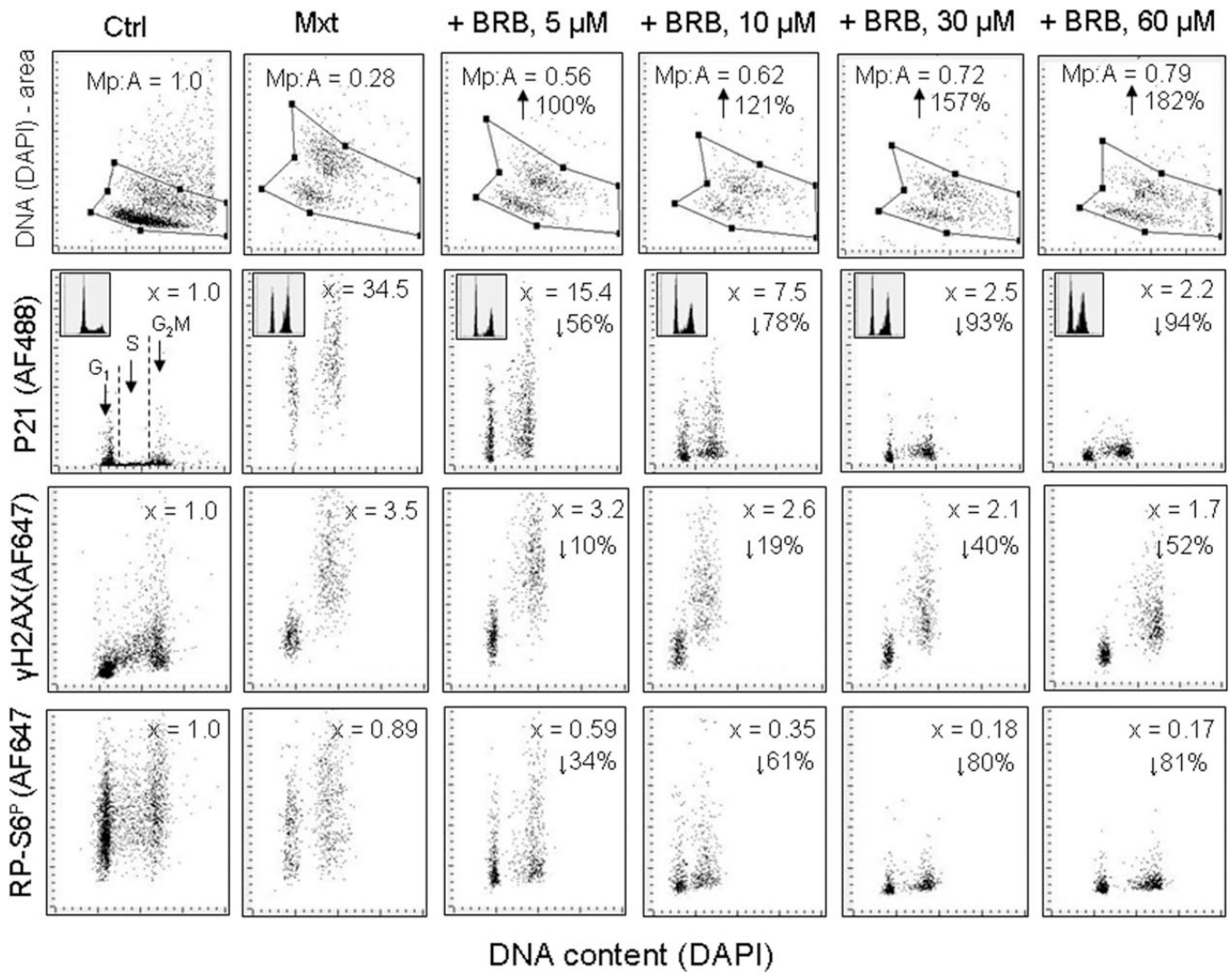

Figure 8.

Attenuation of Mxt-induced senescence of A549 cells by berberine (BRB) as measured by cell morphometric features, expres-sion of $p21^{WAF1}$, γH2AX, and RP-S6P. Exponentially growing A549 cells were untreated (Ctrl) or treated with 2 nM Mxt in the absence and presence of BRB at concentration as shown, for 5 days. Top panels: Morphometric analysis, reporting changes in nuclear area (DNA– DAPI) versus maximal pixel of DAPI fluorescence. The ratio of maximal pixel to nuclear area (Mp:A) is expressed as a fraction of that of the untreated cells; shown also is the percent increase in Mp:A in the BRB-treated cultures with respect to cells growing with Mxt alone (with the arrows). Second horizontal panels: bivariate distributions of p21 versus cellular DNA content; the figures (*x* =) present the increase (*n*-fold) in the mean expression of p21 for all cells with respect to the untreated cells. The percent reduction in p21 in cultures with BRB with respect to Mxt alone is shown with the arrows. Third horizontal panels: expression of γH2AX versus DNA content; the figures (*x* =) represent the increase (*n*-fold) in the mean expression of γH2AX with respect to untreated cells (1.0). The percent reduction in expression of γH2AX in cultures grown with BRB with respect to cells growing in the presence of Mxt alone is presented with the

arrows. Bottom panels: expression of RP-S6^{P} versus DNA content. The figures illustrate the change (*n*-fold) with respect to the untreated (Ctrl) cells. The percent reduction in expression of rpS6^{P} in cultures with BRB with respect to cells treated with Mxt alone is shown with the arrows.

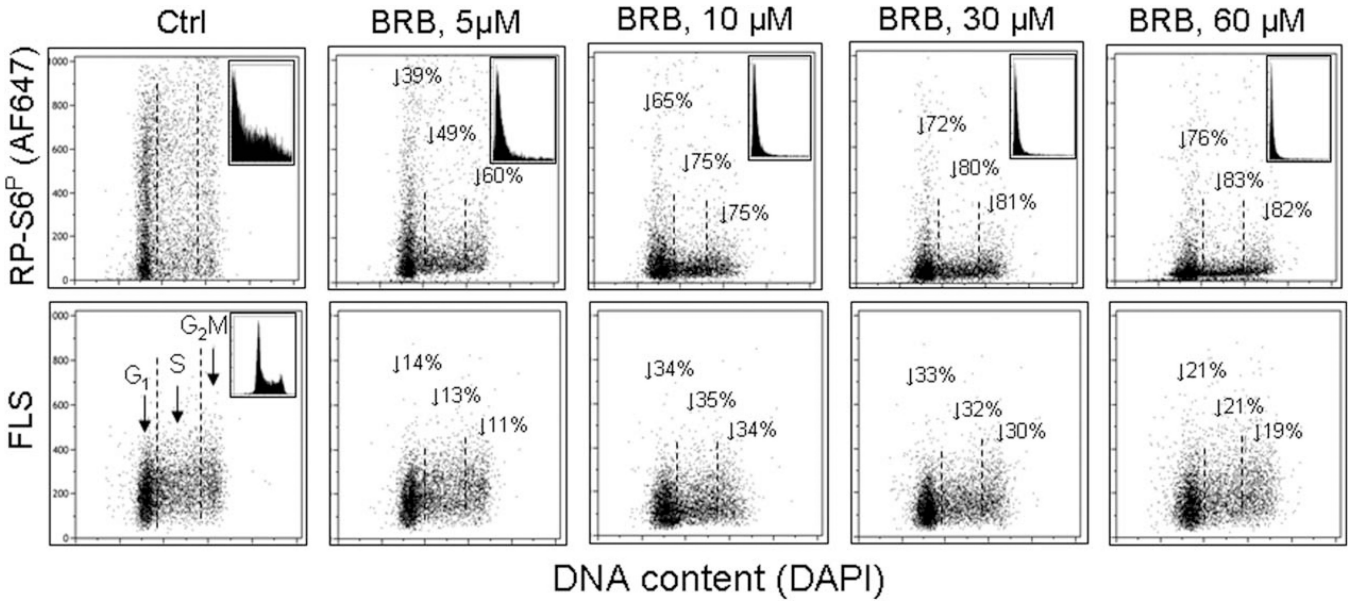

Figure 9.

Suppression of RP-S6 phosphorylation and reduction of size of human lymphoblastoid of TK6 cells maintained at 5–60 μM BRB concentration. Exponentially growing TK6 cells were untreated (Ctrl) or treated with BRB for 24 h. Top panels: the bivariate distributions of RP-$S6^P$ versus DNA content. Figures show percent decrease in expression of the mean RP-$S6^P$ for cells at G_1, S, and G_2M phases of the cell cycle, respectively, in the presence of BRB compared to untreated cells. Insets show the frequency histograms of RP-$S6^P$ expression for all cells in culture. Bottom panels: Bivariate distributions of cellular forward light scatter (FLS) versus DNA content. Percent reduction of mean value of forward light scatter FLS of G_1, S, or G_2M of cells growing in the presence of BRB with respect to the untreated cells is shown with the arrows.

Table 1

The effect of the gero-suppressive drugs on the level of constitutive expression of mTOR-Ser2448^{P}, RP-S6-Ser235/236^{P}, and 4EBP1-Ser65^{P} (detected by phospho-specific Abs) and their corresponding total proteins, assessed by western blotting (Fig. 5)

AGENT	CTRL	2DG	MF	RAP	BRB	VIT. D3	RSV	ASA
mTOR^{P}	1.00	0.73	0.76	0.89	0.99	0.96	1.51	0.75
m-TOR	1.00	1.45	2.25	1.41	1.04	1.07	3.96	1.44
RATIO	**1.00**	**0.50**	**0.34**	**0.63**	**0.95**	**0.90**	**0.38**	**0.52**
RP-S6^{P}	1.00	0.30	0.48	0.05	0.22	0.48	0.42	0.66
S6	1.00	1.04	0.66	0.9	1.02	0.92	0.96	0.57
RATIO	**1.00**	**0.29**	**0.73**	**0.06**	**0.22**	**0.52**	**0.44**	**1.16**
4EBP1^{P}	1.00	0.49	0.58	0.48	0.49	0.75	1.01	0.97
4EBP1	1.00	1.43	1.54	1.7	1.94	1.66	2.05	1.52
RATIO	**1.00**	**0.38**	**0.38**	**0.28**	**0.25**	**0.45**	**0.45**	**0.64**

The figures present the change in expression of the respective proteins in the drug-treated cultures with respect to the untreated ones. Densitometric quantification of phosphorylated and total proteins for mTOR, RP-S6, and 4EBP1 are presented as the “ratio” of actin-normalized phosphorylated to total protein level of expression (bold font).